An Application of Parameter Optimization to Hydraulic Servo Design

G. G. EVANS*
General Electric Company, Schenectady, N.Y.
H. E. VIGOUR†
General Electric Company, Waynesboro, Va.
AND
F. J. ELLERT‡
General Electric Company, Philadelphia, Pa.

This paper describes the use of a parameter optimization method for the design of hydraulic servos. These servos are employed in a two-dimensional contouring control system for a machine tool. The design actually is carried out by adjusting five parameters (gains, time constants) of the servo using a hill-climbing procedure. A physical description and a mathematical model of the hydraulic servo and the associated machine tool are presented. This model includes the amplifiers, stability networks, valves, and hydraulic motor of the servo itself, as well as the inertia, viscous friction, backlash, spring effect, and coulomb friction of the machine tool. Also discussed are the important performance requirements arising from the desire for accurate machining of complex shapes. These requirements stipulate the need for small path errors along the contour and smaller overshoots than undershoots at corners. They are translated into a meaningful performance index, the value of which is to be minimized by the parameter optimization method. The digital computer program and the optimization procedure for the five free servo parameters are discussed. Finally, the path error along a test contour is presented for both the starting and optimum values of the five adjustable parameters. These data indicate clearly the improvement in performance which can be achieved over a servo design carried out by a conventional design method.

Nomenclature

e_p = path error; distance between the actual tool center and the nearest point on the commanded path; in., mils
g_2, g_4 = exponents used in performance index to govern magnitude of penalty for excessive path errors
I = performance index
K_1 = gain of position error amplifier, ma/in.
K_3 = gain of the valve amplifier, ma/v
L_m = leakage coefficient of the motor and the motor metering valve, (in.^{3}/sec)/psi
t = clock time, sec
T_B = torque produced by viscous friction in gearbox, etc., during transients; provides damping to servo, in.-lb
T_D = demand torque, in.-lb
t_f = time at which cutting tool first reaches end of commanded path, sec
T_M = motor torque available to accelerate load inertia, in.-lb
T_1, T_2 = time constants associated with lag break and with lead break, respectively, of servo lag-lead network, sec
x = response of x servo to x_c, in.
x_a, x_b = defines region at top of circular arc of test contour where special emphasis is placed on reducing path errors, in.
x_c = command signal to the x servo, in.
x_d, y_d = coordinates of the point of the commanded path which is nearest to the actual tool center at x, y, in.
y = response of y servo to y_c, in.
y_c = command signal to the y servo, in.
θ_D = one-half of total backlash between motor and load, rad
θ_L, θ_M = angular positions of load and motor, rad
ϕ_i = weighting factors used in the performance index, i = 1, 2, 3, 4

Presented at the AIAA Joint Automatic Control Conference, Seattle, Wash., August 17–19, 1966 (no paper number; published in bound volume of conference papers); submitted December 7, 1966; revision received July 27, 1967. The authors wish to thank D. N. Ewart of General Electric's Electric Utility Engineering Operation for his generous and valuable contribution to the digital computer program and W. A. Lanza of the General Electric Research and Development Center for his suggestions pertaining to the hydraulic servo model. [6.03,8.07]

* System Analysis Engineer, Research and Development Center.
† Senior Development Engineer, Specialty Control Department.
‡ Manager, Electronics, Information and Control, Laboratory Operation, Power Transmission Division.

I. Introduction

THE design of a high-performance servo drive for a machine tool application, such as contouring, requires the consideration of many nonlinearities. These may include multiple saturations in the servo itself as well as backlash, coulomb friction, stiction, etc., in the machine tool. As a result, to obtain good system performance, design techniques must be employed which allow the engineer to take into account the effects of the significant nonlinearities.

Unfortunately, the classical method of design using Bode diagrams and describing functions becomes extremely tedious, if applicable at all, when multiple nonlinearities are present in conjunction with frequency-dependent elements. Also, in such a case, it is difficult for the engineer to relate the frequency domain behavior of the system to the time domain specifications concerned with undershoot and overshoot errors at corners along a typical contour.

A more practical approach is to utilize an analog computer and manually adjust the free system parameters (gains, time constants, etc.) to obtain acceptable performance. The analog computer permits an accurate representation of the system including the nonlinearities. Also, the influence of each adjustable system parameter on the system per-

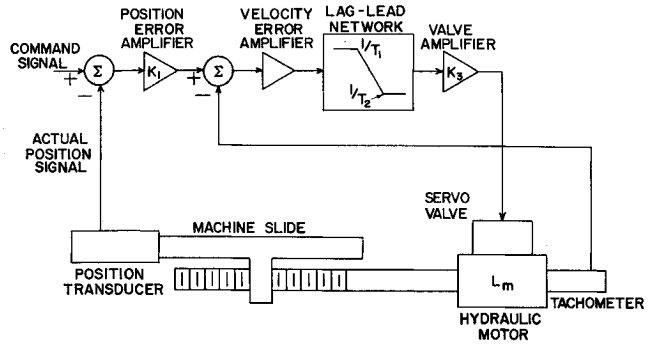

Fig. 1 Schematic diagram of hydraulic servo.

formance is readily obtained. However, the use of the analog computer in this manner can become tedious if a large number of free parameters are to be selected or stringent performance specifications are to be met.

Undoubtedly, the most efficient method, from the viewpoint of the engineering time or elapsed time required, is to employ a digital computer program which automatically selects the free parameters so as to achieve satisfactory performance. The digital computer program permits an accurate representation of the system and can be made to select the adjustable system parameters in a very logical and expeditious manner. For these reasons, the development of such a computer program was undertaken. This program and its application to a typical design are described in this paper.

II. Description of Physical System

The contouring control system treated in this paper consists of two independent hydraulic servo drives which move the tool parallel to the two principal axes of the machine. Separate position command signals are supplied to the servos as continuous functions of time from a command generator, which coordinates the signals so as to command the tool to follow the desired two-dimensional path at the desired speed. Figure 1 shows schematically the essential parts of one of the two servos, which for simplicity were assumed to be identical.

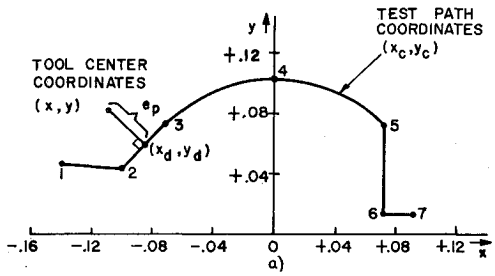

a)

PATH SEGMENT	TIME t (SECONDS)	TEST PATH COORDINATES x_c (t) (INCHES)	y_c (t) (INCHES)
1-2	0 - 0.1	-0.140255 + 0.399452 t	0.045834 - 0.020936 t
2-3	0.1 - 0.2	-0.100310 + 0.282843 (t-0.1)	0.043741 + 0.282843 (t-0.1)
3-5	0.2 - 0.6	-0.101859 COS (3.926991 t)	0.101859 SIN (3.926991 t)
5-6	0.6 - 0.75	0.072025	0.072025 - 0.4 (t - 0.6)
6-7	0.75 - 0.8	0.072025 + 0.4 (t - 0.75)	0.012025

b)

Fig. 2 a) Test path. b) Test path coordinates.

At the upper left, a feedback signal indicating the actual position of the tool is subtracted from the command signal to obtain a position error signal. This signal, after modification by amplifiers and an electrical lag-lead network, acts through a two-stage servo valve to control a constant-displacement hydraulic motor. An inner velocity loop, employing a velocity signal from a tachometer coupled to the motor, regulates motor speed to be proportional to position error. An adjustable needle valve is connected across the hydraulic motor for adjustment of its response characteristics. The motor actuates the machine slide through a mechanism in which backlash and springiness are present to some degree. These mechanical characteristics are included in the position control loop because the position feedback signal is obtained from a transducer connected directly to the machine slide. The parameters to be selected in making the design are identified as K_1, T_1, T_2, K_3, and L_m. The detailed mathematical model of the servo drive, which is required by the design method to be used, is described in Sec. III. A.

Contouring performance was evaluated by commanding the tool center to move at a constant speed of 24 in./min along a typical test path and computing the path error e_p, defined as the distance between the actual tool center and the nearest point on the commanded path. This method of performance evaluation is directly related to the ability of the machine to make accurate parts. Although any path error is undesirable, certain forms of path error are regarded as more serious than others. These are most readily described in connection with the test path shown in Fig. 2. This path includes a circular arc at whose center (point 4) the y axis drive is required to reverse direction slowly. In practice, this slowly reversing command in combination with mechanical backlash and load friction can produce a noticeable flat spot on the workpiece, and special attention was given to reduce path error in this region. The test path also includes sharp corners where servo transients tend to produce larger path errors. In some machining situations involving corners, overshooting on the outside of the corner (as at point 5 or 2) is more serious than undercutting the corner. Consequently, overshoot errors were selectively weighted in relation to undershoots. Figure 3 lists certain values of path errors used as goals in the formulation of the performance index. These are not specification limits, but indicate the relative importance assigned to corner overshoots and undershoots, and flat spots on an arc, in a hypothetical application of the contouring machine. The formulation of an appropriate performance index from these goals is described in the next section.

III. System Model and Performance Index

A. Hydraulic Servo Model

When a digital computer is to be used as a design aid to select automatically the values of the adjustable system parameters, it is essential that an accurate model of the physical system be formulated. Figures 4 and 5 show the model used in this application to simulate the action of the hydraulic servos described in the previous section.[1] Since the x servo and the y servo are assumed to be identical in the physical system, the same model is used for both servos.

MAXIMUM CORNER OVERSHOOT	0.00032 IN.
MAXIMUM CORNER UNDERSHOOT	0.00250 IN.
MAXIMUM VELOCITY ERROR ($\dot{x}-\dot{x}_d$ OR $\dot{y}-\dot{y}_d$)	0.2 IN./SEC.
MAXIMUM ARC OVERSHOOT OR UNDERSHOOT (AT THE TOP OF THE ARC)	0.00020 IN.

Fig. 3 Performance goals for use in performance index formulation.

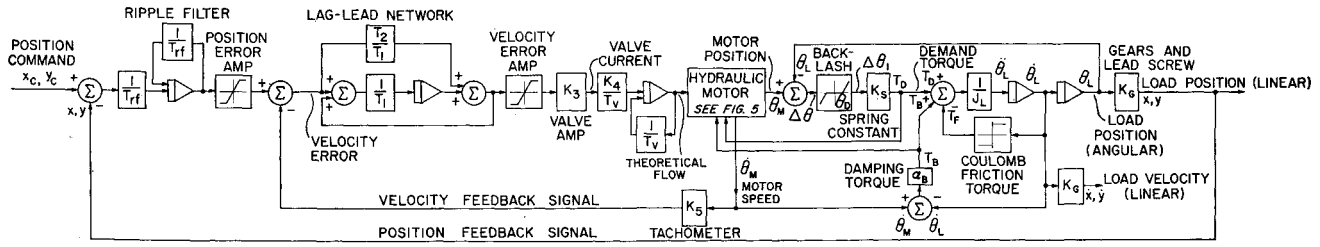

Fig. 4 Mathematical model of hydraulic servo system.

As shown on Fig. 4, the servo yields an output position in response to an input position command. This output is the actual position of the cutting tool. In addition to the outer position feedback loop, the servo contains an inner velocity feedback loop. This inner loop is employed to obtain stability when a high loop gain is used to achieve the high positional accuracy demanded of the system.

The position command signal, either x_c or y_c, is the input to the hydraulic servo model. This command signal is compared to the linear position output, x or y, the difference being the position error signal. After passing through the ripple filter and being amplified, the position error is modfied by the velocity feedback signal from the hydraulic motor to form the velocity error signal to the lag-lead network. This network is necessary to achieve both position loop and velocity loop stability simultaneously with greater steady-state accuracy.

The output of the lag-lead network, after amplification in the velocity-error amplifier and the valve amplifier, becomes the valve current in the flow-control valve. Theoretical flow is the output of the flow-control valve and is the input signal to the hydraulic motor. The mathematical model of the hydraulic motor is shown in Fig. 5. After passing through the flow limiter this theoretical flow is further modified by the multiplier to include the effect of motor back pressure on the actual flow through the valve. Two forms of modification are possible in the model. The multiplication factor could be a function of the motor differential pressure and the supply pressure or this factor could be a fixed quantity. The later option was used to obtain the results given in this paper. The resultant actual flow to the hydraulic motor generates T_M, the motor torque. This is the torque available to accelerate the load inertia which is considered to be coupled to the motor via a springy shaft with backlash present.

For the purpose of the computer simulation, the backlash is considered to occur between the motor position θ_M, and the load position θ_L. Therefore, when both the motor and load positions are increasing and the backlash is taken up in the positive direction, the load position is given by

$$\theta_L = \theta_M - \theta_D \tag{1}$$

where θ_D is equal to one-half of total backlash in radians. Similarly, when both the motor and load position are decreasing and the backlash is taken up in the negative direction, the load position is given by

$$\theta_L = \theta_M + \theta_D \tag{2}$$

Whenever the motor reverses direction, the motor position must change by the amount $\pm 2\theta_D$ before the backlash is taken up and the load position can again follow the motor position according to (1) or (2). This behavior is represented in the computer simulation by calculating the difference quantity $\theta_M - \theta_L$ and applying this difference as an input to a box exhibiting a total deadband of $2\theta_D$ as shown in Fig. 4. As a result, the demand torque T_D applied to the load is zero until $\theta_M - \theta_L$ exceeds $\pm\theta_D$. This agrees with the actual physical behavior because the motor does not accelerate the load until the backlash is taken up. Once this has occurred, the torque T_D is felt by the motor and only the difference torque $T_M - T_D$ is available to overcome the inertia and viscous friction of the motor itself. The torque T_B, which is a torque produced by the viscous friction in the gearbox, etc., during transients when the angular velocities of the motor and load are not equal, is zero after the backlash is taken up. This torque provides damping to the servo.

The demand torque T_D, in conjunction with the damping torque T_B, is applied to the inertia and coulomb friction of the load resulting ultimately in the angular load position, θ_L. Finally the angular load position is converted into the linear load position, x or y, by the gears and lead screw.

This model clearly indicates the multiple nonlinearities present in the servo. As indicated earlier, it is these nonlinearities in conjunction with the stringent performance specifications that make the selection of the adjustable servo parameter values difficult. In this case, there are five such parameters, namely: K_1, the gain of the position error amplifier; K_3, the gain of the valve amplifier; T_1, the time constant associated with the lag break of the lag-lead network; T_2, the time constant associated with lead break of the lag-lead network; and L_m, the leakage coefficient of the motor and the motor metering valve. The hill-climbing procedure is utilized to select the values of these parameters.

B. Performance Index

The hill-climbing procedure adjusts these parameters by an interative, computational method so as to progressively reduce the value of a so-called performance or error index.

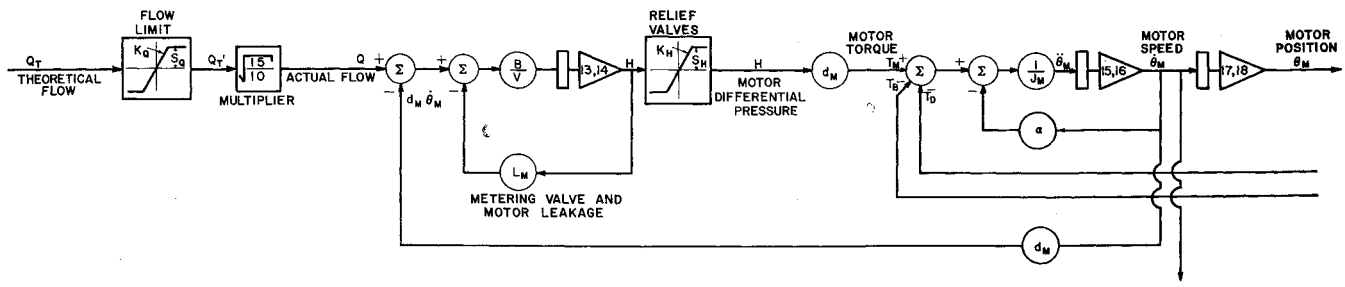

Fig. 5 Mathematical model of hydraulic motor.

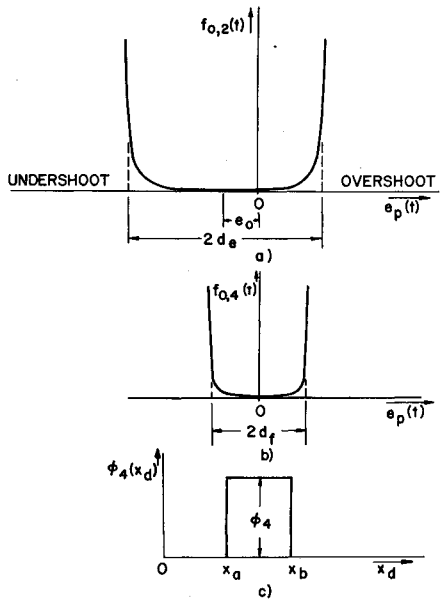

Fig. 6 a) Penalty term to reduce overshoot and undershoot errors. b) Penalty term to reduce errors at the top of the circular test path segment. c) Weighting factor for use with penalty term in b.

This index is derived from the system performance goals of Fig. 3. Good system performance would consist of the following: 1) very small path errors along the straight and circular segments of the test path shown in Fig. 2a, 2) much smaller overshoots than undershoots at corners on the test path, 3) no oscillations due to backlash, or inadequate system damping, and 4) little or no flat region at the top of the circular segment (point 4 in Fig. 2a). These performance requirements are readily translated into a meaningful performance index.[2]

Because the performance of the servo over the entire test path is important, the performance index I is taken to be

$$I = \int_0^{t_f} f_0(t)dt \tag{3}$$

where $f_0(t)$ is the sum of terms related to the performance requirements stated previously and t_f is the time at which the cutting tool first reaches the values of x corresponding to point 7 on the test path, as shown in Fig. 2a.

In order to reduce path errors e_p, a quadratic error term of the following form is included in $f_0(t)$:

$$f_{0,1}(t) = \phi_1[e_p(t)]^2 \tag{4}$$

In this expression, ϕ_1 is a constant weighting factor which is selected by the engineer to place greater or lesser emphasis on this type of error relative to the others to be included in the index.

The quadratic term places equal emphasis on positive and negative path errors and tends to permit large errors as long as they persist for only short intervals of time. In order to reduce the transient path errors at corners and also stress the desirability of smaller overshoots than undershoots, a nonsymmetrical penalty term is included in $f_0(t)$. The form of this term is

$$f_{0,2}(t) = \phi_2\{[e_p(t) - e_0]/d_e\}^{2g_2} \tag{5}$$

This term is depicted in Fig. 6a. As shown, e_0 provides the nonsymmetry with respect to overshoots and undershoots, $2d_e$ specifies the width of the low penalty region, and the exponent g_2 governs the magnitude of the penalty for path errors in excess of those considered acceptable. In order to achieve a sufficiently high penalty for excessive errors, $2d_e$ is set equal to 85–95% of the sum of the maximum allowable overshoot and undershoot errors as stated in the performance goals of Fig. 3. The value of e_0 is obtained from

$$e_0 = 0.9/2[\text{max. allowable overshoot} - \text{max. allowable undershoot}] \tag{6}$$

In order to eliminate oscillations due to backlash or inadequate system damping, the following term is included in $f_0(t)$:

$$f_{0,3}(t) = \phi_3\{[\dot{x}(t) - \dot{x}_d(t)]^2 + [\dot{y}(t) - \dot{y}_d(t)]^2\} \tag{7}$$

In this expression, $\dot{x}(t)$ and $\dot{y}(t)$ are the rectangular components of the computed tool velocity, while $\dot{x}_d(t)$ and $\dot{y}(t)$ are the velocities desired at the point x_d, y_d on the test path, as shown in Fig. 2a. If oscillations occur for one set of the adjustable servo parameters, these velocity difference terms will become quite large even though the path error term of (4) may not. Hence, in attempting to reduce the value of the performance index, the hill-climbing procedure will select new sets of adjustable parameters which reduce and ultimately eliminate the oscillation.

In order to reduce the potential flat region at the top of the circular segment of the test path, the following term is included in $f_0(t)$:

$$f_{0,4}(t) = \phi_4(x_d)[e_p(t)/d_f]^{2g_4} \tag{8}$$

This is a symmetrical penalty term with a weighting factor which is a function of the x component of the desired tool position on the test path. This penalty term and the weighting factor $\phi_4(x_d)$ are shown in Figs. 6b and 6c, respectively. By means of this weighting factor, it is possible to place emphasis on the path error in a particular region along the test path. Therefore, to reduce errors just beyond the top of the circular segment, x_a is set equal to the value of x_d corresponding to point 4 in Fig. 2a. The quantity x_b then is selected to be larger than x_a by a sufficient amount to cover the region during which the undesirable flattening usually occurs. The value of d_f is taken to be 90% of the allowable error associated with the flat.

The complete performance index then becomes

$$I = \int_0^{t_f} [f_{0,1}(t) + f_{0,2}(t) + f_{0,3}(t) + f_{0,4}(t)]dt \tag{9}$$

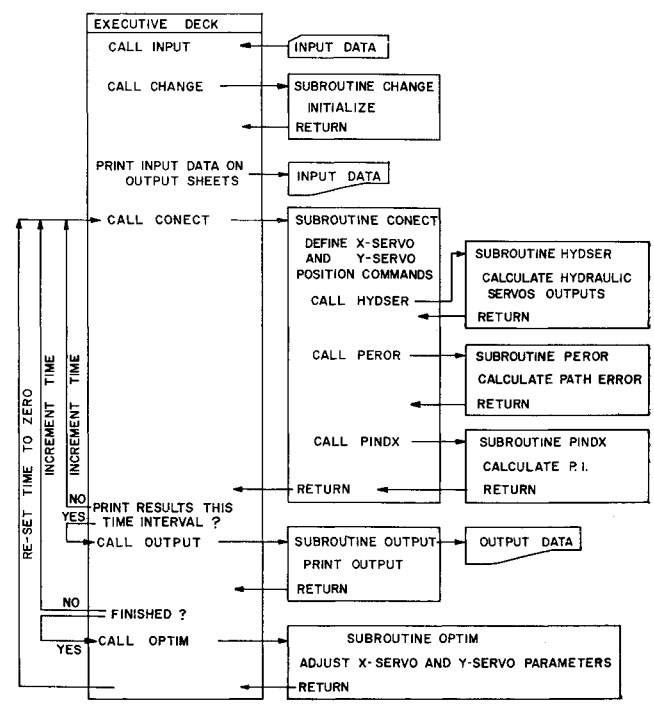

Fig. 7 Block diagram of computation cycle.

Without loss of generality, one of the weighting factors may be set equal to unity. The remaining weighting factors then are selected such that each term contributes essentially equally to the value of the performance index. Further adjustments in these weighting factors usually are necessary during the initial iterations on the computer.

IV. Digital Computer Program

The digital computer program utilized to select the adjustable servo parameters is composed of several subroutines. In block diagram form, Fig. 7 shows the various subroutines, how they are interconnected, and the general computational sequence.

The true contour, which the x servo and y servo are attempting to reproduce, is shown in Fig. 2a. The coordinates of this contour, x_c and y_c, become the position command signals or inputs to these servos as functions of time. The mathematical expressions for these input position commands are given in Fig. 2b. Also given in Fig. 2b is the ideal time required by the cutting tool to traverse each segment of the specified contour. These times are based on a linear contouring rate of 0.4 in./sec. Because the performance of the servos is not perfect, the actual traverse time of each segment of the contour will be longer than that listed in the table.

Using the position command signals described previously, the response of both hydraulic servos is computed. At any instant of time, the position outputs of the two servos represent the actual position of the cutting tool. This tool position is designated x, y. At each instant of time the program computes x, y in subroutine HYDSER using the mathematical model described previously to represent the servos. Inherent in the computation of the cutter position x, y using the servo model is the computation of $\dot{x}$ and $\dot{y}$, the time derivatives of x and y, respectively. These linear velocities are needed for the evaluation of the performance index.

As the coordinates x, y change in response to the position commands, the cutting tool should trace the desired contour. At any instant of time, it is unlikely that the cutter position x, y is exactly a point on the specified contour. A subroutine, PEROR, is used to calculate the instantaneous deviation of the cutter position from the desired contour. This instantaneous deviation is termed the path error e_p, and is defined as the perpendicular distance from the cutter position to the true contour. Subroutine PEROR also calculates x_d, $\dot{x}_d$, y_d, and $\dot{y}_d$. Having e_p, x_d, $\dot{x}_d$, $\dot{y}_d$, and y_d from subroutine PEROR and x and y from subroutine HYDSER, the performance index is computed in subroutine PINDX.

Next, subroutine OPTIM determines those values of the five adjustable servo parameters that will yield the optimum (minimum) value of the performance index. The engineer must specify initial values for the five parameters to define the first base point. At this base point a gradient is calculated. This is the direction of greatest change in the performance index. A step is taken in this direction to yield a new base point. A new gradient is computed and another step taken. This process is repeated until the minimum value of the performance index is obtained. It is best described by reference to Fig. 8.

When entered for the first time, subroutine OPTIM initializes on the basis of the input data. The first adjustable parameter is then perturbed a prescribed amount. All other adjustable parameters remain at their base point values. Subroutine OPTIM then returns to the main program, the performance index is calculated for this new set of parameters, and the program returns to subroutine OPTIM. OPTIM then calculates the required partial derivative for the first adjustable parameter from

$$\partial I/\partial K_1 = \Delta I/\Delta K_1 \qquad (10)$$

where ΔI is the change in the performance index resulting from the perturbation ΔK_1 in the first adjustable parameter. In sequence, all of the adjustable parameters are perturbed and the corresponding partial derivatives determined. Using these partial derivatives, the direction of the greatest change in the performance index is determined and a new value is calculated for each adjustable parameter so as to produce a desired change in the value of the performance index. This new set of parameters defines a new base point and a corresponding value for the performance index.

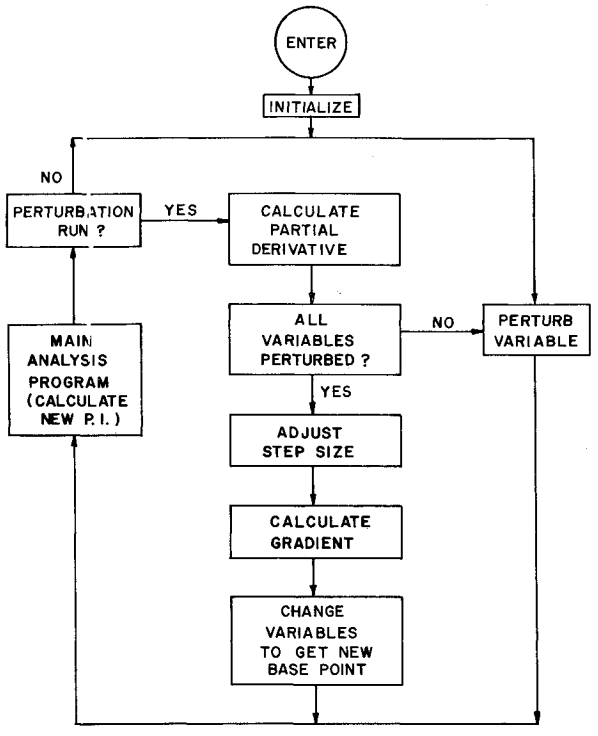

Fig. 8 Block diagram of parameter optimization method.

This procedure is then repeated. However, for all base points after the first one, the actual and desired changes in the performance index from the preceding base point also influence the amount by which each parameter is adjusted. The greater the improvement in the value of the index, the greater the increase in step size. If the performance index remains unchanged, so does the step size. If the performance index worsens, the step size is decreased. Using the computed partial derivatives and the adjusted step size, new values for each of the adjustable parameters are calculated to obtain a new base point. Following this, the entire process is repeated.

V. Computed System Performance

In the computation of the system performance, all parameters of the hydraulic servos (see Figs. 4 and 5), with the exception of the five adjustable parameters, remain fixed at the following values:

S_Q = 38.4 in.^{3}/sec
S_H = 2200 psi
K_4 = 2.56 in.^{3}/sec-ma
K_5 = 0.00318 ma/rad-sec
K_G = 0.0177 in./rad
K_H = 1
K_Q = 1
K_S = 18,300 in.-lb/rad
B = 200,000 psi
V = 1.35 in.^{3}
J_M = 0.220 in.-lb-sec^2
J_L = 0.0183 in.-lb-sec^2
d_m = 0.16 in.^{3}/rad

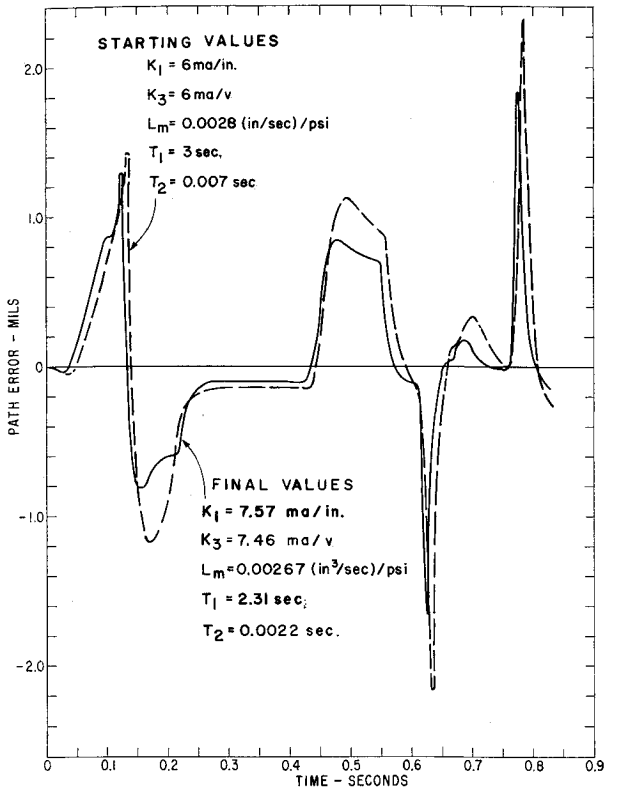

Fig. 9 Path error using starting values and optimum values for adjustable parameters.

$\alpha = 0.21$ in.-lb/rad-sec
$\alpha_B = 10$ in.-lb/rad-sec
$\theta_D = 0.113$ rad
$T_F = 20$ in.-lb
$T_{rf} = 0.004$ sec
$T_V = 0.002$ sec

A set of values also was selected for the parameters of the performance index. During the initial runs on the computer, these values were adjusted to provide the desired trade-off between the various error terms in the index. The values used for all subsequent computer runs are as follows:

$\phi_1 = 0.964506 \times 10^6$ $\quad e_0 = -0.000981$
$\phi_2 = 0.08$ $\quad d_e = 0.001269$
$\phi_3 = 1.0$ $\quad x_a = 0.0$
$\phi_4 = 39.574 \times 10^{-9}$ $\quad x_b = 0.056$
$g_2 = 3.0$ $\quad d_f = 0.00018$
$g_4 = 5.0$

The positions of the x servo and the y servo are assumed to be correct to start the problem. That is, the proper initial conditions were placed on the motor and load position integrators (see Fig. 4) so that a steady-state start is made from point 1 in Fig. 2a.

The initial, or starting, values for the five adjustable servo parameters, obtained using classical servo design methods, are given in Fig. 9. This figure shows the resulting path error in mils for these starting values.

After completion of the optimization, the values of the five adjustable parameters are given in Fig. 9. The resulting path error in mils for these values also is shown.

Inspection of Fig. 9 shows that the path error e_p has six distinct peaks, four positive and two negative, occurring at $t = 0.13$, 0.17, 0.49, 0.63, 0.70, and 0.78 sec. Comparison of path errors when using starting values for the adjustable parameters with path errors when using optimum values reveals that every one of these six peaks has been reduced by the use of the optimized values for the five parameters being adjusted. The peak path error values for the initial and optimized parameter values are summarized in Table 1. These are actual values taken from the tabulated results used to plot Fig. 9.

For this application, overshoot and undershoot errors are defined in Table 2. "Tool left" means that the actual tool position (x, y) lies to the left of the commanded path as seen by an observer looking along the commanded path in the direction of the command motion. Thus, of the six peak values of e_p listed, the second, third, and fifth are overshoot errors whereas the remainder are undershoot errors.

Note that the greatest percent reductions in the path errors have occurred in the overshoot errors. This is exactly as intended, since $f_{0,2}(t)$ of the performance index was formulated to emphasize the reduction of overshoot errors at the second and fifth data points, while $f_{0.4}(t)$ was formulated to reduce path errors in the region of the third point.

VI. Conclusions

The computed system performance indicates that a worthwhile improvement in performance can be achieved using this method based on parameter optimization. Of course, the degree of improvement is very much a function of the starting values selected for the adjustable parameters. In this study, a reasonably thorough design was made using linear control theory to arrive at these starting values. Actually, in order to utilize this design tool most effectively, very little engineering time should be devoted to the selection of the starting values. The tedious task of adjusting these values should be left to the computer.

A further reduction in the peak errors might still be obtained by modifying the performance index parameters. Once the best tradeoff has been achieved between the various errors, the performance index parameters could be fixed and utilized for all production designs of a given class of hydraulic servos.

This study is regarded as an important step in increasing the engineer's ability to optimize the design of contouring systems. However, a design of this kind is not routinely made for applications where experience with similar machines indicates that the use of a conventional design method is adequate. For difficult cases, however, where the performance requirements are stringent and where data can be obtained concerning the machine nonlinearities, the design method described here should prove valuable.

One further degree of sophistication is possible in the design of contouring control systems. In addition to optimizing the gains and time constants of the servos, it also is possible to optimize the position command signals. This would result in the introduction of anticipation into these signals so that the servos would be commanded to begin the turn for a corner before the corner actually should be machined. In this way, the lags in the servos would be partially compensated for by the anticipation in the commands. These modified command signals with anticipation can be

Table 1 Reduction of path error peaks using optimum parameter values

Initial parameter values		Optimized parameter values		
Time, sec	Path error, mils	Time, sec	Path error, mils	Percent reduction
0.130	1.432	0.124	1.270	11.3
0.169	−1.172	0.155	−0.816	30.4
0.491	1.122	0.479	0.841	25.0
0.632	−2.142	0.625	−1.660	22.5
0.700	0.343	0.688	0.182	46.9
0.781	2.323	0.774	1.838	20.9

Table 2 Overshoot and undershoot errors

t, sec	Tool left	Tool right
0–0.2	Undershoot	Overshoot
0.2–0.75	Overshoot	Undershoot
0.75–end	Undershoot	Overshoot

generated using dynamic optimization techniques which have been widely discussed in the literature.[3]

References

[1] Lewis, E. E. and Stern, H., *Design of Hydraulic Control Systems* (McGraw-Hill Book Company Inc., New York, 1962).

[2] Ellert, F. J., "Indices for control system design using optimization theory," Doctoral Thesis, Rensselaer Polytechnic Inst., Troy, N.Y. (January 1964).

[3] Merriam, C. W., III, *Optimization Theory and the Design of Feedback Control Systems* (McGraw-Hill Book Company Inc., New York, 1964).

NOVEMBER 1967 J. SPACECRAFT VOL. 4, NO. 11

Calculated Aeroelastic Bending of a Sounding Rocket Based on Flight Data

GEORGE E. REIS* AND WAYNE D. SUNDBERG†
Sandia Laboratory, Albuquerque, N. Mex.

During a series of Nike-Tomahawk sounding rocket flights, large extra-atmospheric coning angles were observed which were not predicted by preflight calculations. The most probable causes were concluded to be Magnus forces, aeroelastic bending, and/or lee-side boundary-layer separation. This paper is a report of an investigation of the aeroelastic behavior of one of these flights. An analysis was made which assumed that the missile consisted of two rigid bodies (payload and motor) hinged at their interface. Three-degree-of-freedom moment equations were written for each of the sections that were coupled by a bending moment at the hinge point. Sufficient data were available from flight, wind-tunnel, and laboratory tests to calculate the coning angles of each section. The maximum angular difference between the payload and the motor, immediately following second-stage burnout, was calculated to be $\frac{3}{4}°$. Flexural strengths obtained from bending tests accounted for the angular difference except for a 4-sec period near burnout. The additional bending is attributed to the opening of the payload separation joint caused by the rapid aerodynamic heating and sudden loss of acceleration at second-stage burnout.

Nomenclature

d = missile diameter, ft
I_{xn}, I_{yn} = moments of inertia of the payload about the x and y axes, respectively, in the payload coordinate system, slug-ft²
I_{xt}, I_{yt} = moments of inertia of the motor about the x and y axes, respectively, in the motor coordinate system, slug-ft²
K = payload-motor elastic flexural stiffness coefficient, rad/ft-lb
M_{bn} = hinge bending moment applied to the payload by the motor at the payload-motor joint, ft-lb
M_{xn}, M_{xt} = external moments applied about the x axes of the payload and motor, respectively, in their individual coordinate systems, ft-lb
$M_y(\theta_n), M_y(\theta_t)$ = aerodynamic moments applied about the y axes of the payload and motor, respectively, in their individual coordinate systems due to their respective angles of attack, ft-lb
$M_y(\dot{\theta}_n), M_y(\dot{\theta}_t)$ = aerodynamic moments applied about the y axes of the payload and motor, respectively, in their individual coordinate systems, due to the rate of change of their respective angles of attack, ft-lb
M_z = $M_{zn} + M_{zt}$, sum of the external moments applied about the z axes of the payload and motor, respectively, in their individual coordinate systems, ft-lb
q = dynamic pressure = $\rho V^2/2$, psf
V = missile velocity, fps
x, y, z = orthogonal body coordinates
X = distance between point P in Fig. 1 and the center of pressure of the payload section, ft
θ_n, θ_t = payload and motor coning angles, respectively, rad; these are assumed to equal their respective angles of attack
ρ = air density, slug/ft³
ρ_{62} = air density taken from Ref. 8, slug/ft³
ω_s = $\omega_s' - \omega_p \cos\theta_n$, rad/sec
ω_s' = inertial spin rate about the x axis, rad/sec
ω_p = missile coning rate, rad/sec

Presented at the AIAA Sounding Rocket Vehicle Technology Specialist Conference, Williamsburg, Va., February 27–March 1, 1967 (no paper number; published in bound volume of conference papers); submitted March 13, 1967; revision received July 14, 1967. The authors would like to thank W. B. Brooks for the suggestion to treat the missile as a two-body problem. This work was supported by the Atomic Energy Commission. [7.02, 7.08]

* Staff Member, Aero-Thermodynamics Department.

† Staff Member, Aero-Thermodynamics Department. Associate Member AIAA.

Introduction

OVER the past four years, a series of Nike-Tomahawk[2] sounding rockets with a variety of payloads has been launched by Sandia Laboratory. Preflight estimates of the behavior of the spinning missile in flight were made using a six-degree-of-freedom computer program. The observed